Talanta 185 (2018) 281–290

Contents lists available at ScienceDirect

Talanta

journal homepage: www.elsevier.com/locate/talanta

Specific detection of stable single nucleobase mismatch using SU-8 coated silicon nanowires platform

Melania Banu[a,b,*], Monica Simion[a,**], Marian C. Popescu[a], Pericle Varasteanu[a,c], Mihaela Kusko[a], Ileana C. Farcasanu[b,d]

[a] National Institute for Research and Development in Microtechnologies – IMT Bucharest, 126 A Erou Iancu Nicolae Street, 077190 Bucharest, Romania
[b] Faculty of Biology, University of Bucharest, 91-95 Splaiul Independentei Avenue, 050095, Bucharest, Romania
[c] Faculty of Physics, University of Bucharest, 405 Atomistilor Street, 077125 Magurele, Romania
[d] Faculty of Chemistry, University of Bucharest, 90-92 Panduri Street, 050663, Bucharest, Romania

ARTICLE INFO

Keywords:
Microarray platform
Silicon nanowires
SU-8
APTES-GAD
BRCA1
Biochip specificity

ABSTRACT

Novel microarray platform for single nucleotide polymorphisms (SNPs) detection has been developed using silicon nanowires (SiNWs) as support and two different surface modification methods for attaining the necessary functional groups. Accordingly, we compared the detection specificity and stability over time of the probes printed on SiNWs modified with (3-aminopropyl)triethoxysilane (APTES) and glutaraldehyde (GAD), or coated with a simpler procedure using epoxy-based SU-8 photoresist.

Scanning electron microscopy (SEM) and energy dispersive X-ray spectroscopy (EDX) were used for comparative characterization of the unmodified and coated SiNWs. The hybridization efficiency was assessed by comprehensive statistical analysis of the acquired data from confocal fluorescence scanning of the manufactured biochips.

The high detection specificity between the hybridized probes containing different mismatch types was demonstrated on SU-8 coating by one way ANOVA test (adjusted p value *** < .0001). The stability over time of the probes tethered on SiNWs coated with SU-8 was evaluated after 1, 4, 8 and 21 days of probe incubation, revealing values for coefficient of variation (CV) between 2.4% and 5.6%. The signal-to-both-standard-deviations ratio measured for SU-8 coated SiNWs platform was similar to the commercial support, while the APTES-GAD coated SiNWs exhibited the highest values.

1. Introduction

DNA microarray technology revolutionized the areas of genetics and molecular biology in the mid 90's by facilitating the simultaneous investigation of the expression levels for thousands of genes, enabling high-throughput analysis [1,2]. Further studies recommended the technique for single nucleotide polymorphism (SNP) genotyping and have a key role in the identification of DNA variants which increase the predisposition to various disorders [3–5]. Improvements in limit of detection down to fM and the enhanced specificity of single base mismatch detection were recently reported [6,7]. The dedicated analysis of thermodynamically stable single nucleotide mismatches was conducted by means of atomic force spectroscopy (AFS) [8] and DNA melting temperature analysis [9].

In microarray, the use of a flat support inhibits the amount of biological samples attached to a chemically modified surface, thus decreasing the sensitivity and specificity of the technique [10–14]. Therefore, three-dimensional (3D) detection platforms became a promising approach for achieving a higher probe binding capacity as compared to the typical two-dimensional substrates [15–18]. Significant enhancement of the detection specificity and sensitivity has been reported on nanostructured quartz [19], polymer-based three-dimensional substrates [20] or three-dimensional dextran matrix covalently coated on glass surface [6]. Among them, silicon-based substrates tailored in customizable geometries through processes applied in microelectronics came into focus due to their specific technological traits: control, reproducibility, stability [21,22]. Silicon nanowires (or black silicon) possess low reflectance capabilities and a broadband light absorption [23–26], characteristics which are essential in microarray applications. Hence, this architecture reduces the autofluorescence due to the multiple reflections on substrate and SiNWs “forest”, enhancing the transmittance due to the coupled guided modes which propagate

* Corresponding author at: National Institute for Research and Development in Microtechnologies – IMT Bucharest, 126 A Erou Iancu Nicolae Street, 077190 Bucharest, Romania.
** Corresponding author.
E-mail addresses: melania.banu@imt.ro (M. Banu), monica.simion@imt.ro (M. Simion).

https://doi.org/10.1016/j.talanta.2018.03.095
Received 4 December 2017; Received in revised form 26 March 2018; Accepted 29 March 2018
Available online 30 March 2018

along the length of SiNWs, thus resulting in improved light absorption and signal intensity.

The most common mechanisms for DNA binding onto a surface (glass, silicon, synthetic polymer) involve chemically-modified probes with amino or thiol nucleophilic groups covalently attached to epoxide, aldehyde, succinimidyl ester or isothiocyanate functionalized substrates [27,28]. Glycidyl ether of bisphenol A (SU-8) is a low-cost epoxy-based photosensitive polymer, thermally and chemically stable, with excellent physical and optical properties, commonly used as negative photoresist in micromachining and microelectronics, suitable for immobilization of bio-molecules in Bio-MEMS and biosensors [29,30]. The feasibility of SU-8 coated glass slides for microarray fabrication by directly immobilizing modified oligonucleotides is already established [31,32]. Sensitive hybridization was achieved on Blu-ray disk coated with SU-8, opening a way to high-density microarrays [33]. However, there are no reports regarding the use of SU-8 on 3D architectures supporting the uniform attachment of DNA probes.

Our previous studies were mainly focused on assessing the discrimination efficiency between perfect-matched (PM) and mismatched sequences (MM) by developing a microarray chip based on silicon nanowires (SiNWs) functionalized with (3-Aminopropyl)triethoxysilane (APTES) and glutaraldehyde (GAD) [34], but the controlled spot size and the long term stability of the tethered probes remained to be settled in order to claim its commercial destination. Starting from the previous findings, we developed herein a new chemically stable biochip for accurate control of the microarray spot sizes by using SU-8 coating of SiNWs, with superior detection specificity and reproducibility. *BRCA1*-corresponding sequences were employed, because any modification - such as single nucleotide polymorphisms - increases the lifetime risk for the development of breast and ovarian cancer [35–38], as revealed by SNP arrays [39]. The perfect complementarity of the *BRCA1* canonical probe sequence (containing the common C allele) with the target molecules and the effect of the mismatches in terms of specificity were analysed by replacing the C nucleotide with another nucleotide (C > A and C > T), or two adjacent nucleobases (CG > AA) generating three other variants of *BRCA1* probe sequences. The replaced single nucleotides form DNA duplexes containing A/G and G/T mismatches which are the most stable among other types of disparities [40], whereas the sequence containing two mismatches was designed to form destabilizing AA/GC duplexes. Negative control probe sequences were also used to certify the appropriate hybridization conditions.

In this article, we report high detection specificity among the hybridized probes containing different mismatch types on SiNWs support covered with SU-8. Accordingly, the hybridization data collected using confocal fluorescence scanning from 320 technical replicates/probe type (PM, C > A and C > T) were normalized. After removing the outliers, the datasets were analysed by one way ANOVA, leading to the adjusted p value *** < 0.0001 which demonstrated the high detection specificity among the hybridized probes containing different mismatch types on the new SU-8 coated SiNWs support. It is notable that the signal-to-both-standard-deviations ratio measured for SU-8 coated SiNWs platform is similar to the commercial support, while SiNWs coated with APTES-GAD display the highest values. Furthermore, we shown a significantly improved stability over time of the probes tethered on this substrate, revealing variation coefficients between 2.4% and 5.6% at our evaluations after 1, 4, 8 and 21 days of probe incubation.

2. Experimental section

2.1. Materials and reagents

Superaldehyde 3 Premium Microarray Substrates were purchased from ArrayIt Corporation (Sunnyvale, USA). The p-type silicon wafers were ordered from SIEGERT WAFER (Germany). The oligonucleotides were provided by Biomers.net (Germany).

SU-8 2002 photoresist was acquired from Microchem (USA). Nuclease-free water and coverslips were purchased from Roth (Germany). Herring sperm DNA was obtained from Promega (USA). Adhesive films for microtiter plates were purchased from EXCEL Scientific (USA). Sterile microtiter plates were acquired from BRAND (Germany). Unless otherwise specified, all the other chemicals were supplied by Sigma-Aldrich (Germany).

2.2. Fabrication of 3D microarray platforms

The generation of SiNWs as 3D substrates employed one-step metal-assisted chemical etching (MACE), where $AgNO_3$ was used as an etching catalyst [41]. As described in our previous study [34], the p-type Si substrates were immersed in 0.06 M $AgNO_3$ and 4.5 M HF, for 40 min in the absence of light. At this point, SiNWs were formed and the chips were dipped into 60% v/v HNO_3 solution for 30 min, in order to remove any residual catalyst and, followed by immersion in 5% v/v HF solution for 1 min.

Two types of SiNWs functionalization were done and their impact on hybridization efficiency and data reproducibility was investigated: (i) the standard APTES-GAD protocol providing the –CHO functional groups (***GAD/SiNWs***); and (ii) the SU-8 coating yielding the epoxy functional groups (***SU-8/SiNWs***). Thus, a set of SiNWs substrates was modified with APTES and GAD, using the optimized protocol previously reported [42]. The other set was dipped into 5% HF for 1 min, cleaned under O_2 plasma for 10 min and covered with SU-8 2002 photoresist, by spinning at 4000 rpm. Afterwards, the *SU-8/ SiNWs* supports were soft baked for 1 min at 65 °C and 2 min at 95 °C, followed by the post-baking performed at 180 °C for 30 min. Unlike the deposition on a standard flat substrate [43], the 3D architecture assured a much thinner deposition due to the uniform polymer dispersal into the substrate, reducing the auto-fluorescence level [32].

2.3. Microarray experiment

The oligonucleotide probes and target sequences used in this study correspond to *BRCA1* gene [44]. The negative control (fully mismatched sequence) and *BRCA1*-specific probes were designed to have a C6 amino-link modification at 5′ end and to contain two types of single nucleotide mismatch in the same locus (Table 1).

The mismatched sequences were designed in accordance with the SNPs reported for the pathogenic allele, available in “The Single Nucleotide Polymorphism Database (dbSNP) of nucleotide Sequence Variation [45,46]. Rs28897696 is a polymorphism which, if found in homozygous form (two copies), is very likely to increase the risk of developing breast or ovarian cancer [47]. A second mismatch corresponding to rs1057520432, with likely benign allele was introduced in one of the probe types in order to generate a stronger destabilizing effect on the duplex. The complementary target sequence had a Cy3 dye

Table 1
Probe and target sequences.

BRCA1		
Perfect Matched Sequence (PM)		5′-*C6-NH_2*-CTAGGAATTGCGGGAGGAAAATGGG – 3′
Sequences with 1 mismatch (MM)	**C > A**	5′- *C6-NH_2*-CTAGGAATTG**A**GGGAGGAAAATGGG – 3′
	C > T	5′- *C6-NH_2*-CTAGGAATTG**T**GGGAGGAAAATGGG – 3′
Sequence with 2 mismatches (2MM)	**CG > AA**	5′- *C6-NH_2*-CTAGGAATTG**AA**GGAGGAAAATGGG – 3
Negative control sequence (**Nc**)		5′-*C6-NH_2*-TTGCATCTTCTGGGTCAGGTACGGA – 3′
Complementary sequence **(C)**		5′-Cy3-CCCATTTTCCTCCCGCAATTCCTAG – 3′

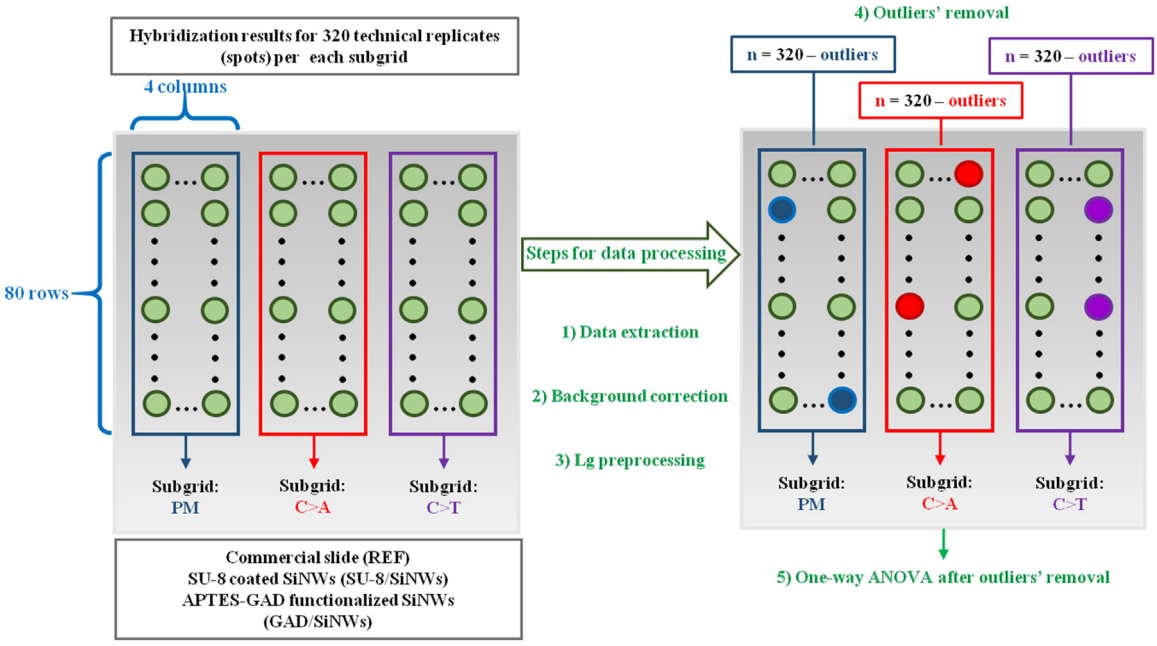

Fig. 1. Layout for PM, C > A and C > T probes spotted on the test supports and data processing steps for statistical analysis.

attached to the 5′ end, necessary for fluorescent detection of hybridization. The immobilization buffer consisting of 200 mM Na_2HPO_4 (sodium phosphate, dibasic), pH 8.5, was used for probes' preparation, subsequently spotted at 50 μM concentration using an Omni Grid Micro Contact printer (Genomic Solutions) with controlled humidity (80%) and temperature (25 °C) in the printer chamber. The spotting, immobilization, washing and blocking conditions were previously established [33,48]. The layout of the probes spotted on the surfaces is presented in Fig. 1. Namely, 3 subgrids of 4 × 80 spots (320 replicates) corresponding to perfect matched (PM), C > A and C > T single mismatches, respectively, were spotted on both aldehyde-modified commercial glass support and the homemade new supports based on SiNWs by using a 200 μm tip. For control experiments, 4 subgrids corresponding to negative control Nc, perfect matched PM, single mismatch C > A and double mismatch CG > AA probes were deposed on aldehyde-modified glass slide, functionalized SiNWs, as well as on functionalized flat Si substrate. Overnight incubation of the supports was done at room temperature, for attaining a covalent bonding of the probes on surface. The removal of unbound probes was subsequently achieved by washing the slides three times successively in each of the following solutions: (i) 2 × SSC/0.1% w/v SDS (saline sodium citrate/sodium dodecyl sulphate); (ii) 1 × SSC; (iii) DIW (deionized water). The blocking of unreacted sites was performed by immersing the microarray platforms for 30 min at 42 °C and 250 rpm in a preheated solution (42 °C) of 1% w/v BSA (bovine serum albumin) in 5 × SSC and 0.1% w/v SDS.

Carefully prepared samples were stored for 1 day and 21 days at 4 °C in N_2 atmosphere before hybridization, aiming to analyse the short- and long-term stability of the platforms, with additional 4 and 8 days intervals dedicated to *SU-8/SiNWs*. An optimized hybridization protocol involved the Cy3-complementary sequences diluted to 10 μM in a buffer preheated to 60 °C, which consisted of 2 × Denhardt's solution, 10 × SSC and 200 μg/mL herring sperm DNA. The hybridization solution was dispersed on the surface by encasing each biochip with a coverslip and the target's evaporation was prevented by incubating the slides in a humid chamber for 4 h at 42 °C. Prior to scanning, the unbound target sequences were discarded by washing the slides for three times successively in 2 × SSC/0.1% w/v SDS, 1 × SSC and DIW.

2.4. Characterization and analysis

2.4.1. Equipments

The morphological imaging and measurements of the as-prepared SiNWs, ***GAD/SiNWs*** and ***SU-8/SiNWs*** microarray substrates were performed with a Field Emission Scanning Electron Microscope (FE-SEM), FEI-NOVA NanoSEM 630. The wettability of the functionalized substrates was determined at room temperature by employing the KSV Theta Optical Tensiometer equipment. Deionized water was used in the sessile drop tests, and the droplet volume was controlled using an automatic dispensing system. Hybridized DNA was detected with a laser scanning confocal fluorescence system (GeneTAC UC4 Microarray Scanner, Genomic Solutions), by scanning the slides with Cy3 (532 nm) excitation laser at 10 μm/pixel. Raw images were imported into GenePix® Pro 7 Software for spot detection and quantification of the intensity of hybridization signal. The acquired data points were not flagged as "bad" at this stage; they were removed afterwards from the graphical and statistical analysis of the mismatches.

2.4.2. Statistical analysis

Datasets based on 320 technical replicates/probe type were generated by GenePix® Pro 7 software for extracting the average signal intensities and the local background intensities, subsequently processed and analysed in RStudio 1.0.136 [49] environment for R 3.4.0, and the microarray layout accompanied by the steps for data processing are illustrated in Fig. 1 [50]. The datasets corresponding to the control experiments were analysed using exactly the same steps applied for the slides containing PM, C > A and C > T. The graphics were generated using background-corrected values, normalized by log10 transformation, to make the data interpretation easier and more meaningful [51]. The values situated 2σ (standard deviation) away from the mean were treated as outliers and removed from the graphical and statistical analysis of the mismatches. All the graphs were generated using ggplot2 R package [52]. For the control experiments engaging Nc, PM, C > A and CG > AA probe types, these datasets were analysed using exactly the same steps applied for the slides containing PM, C > A and C > T.

One way analysis of variance (ANOVA) with Tukey's honestly significant difference (HSD) post hoc tests ($\alpha = 0.05$), available in RStudio was used for the statistical analysis of the hybridization data in control

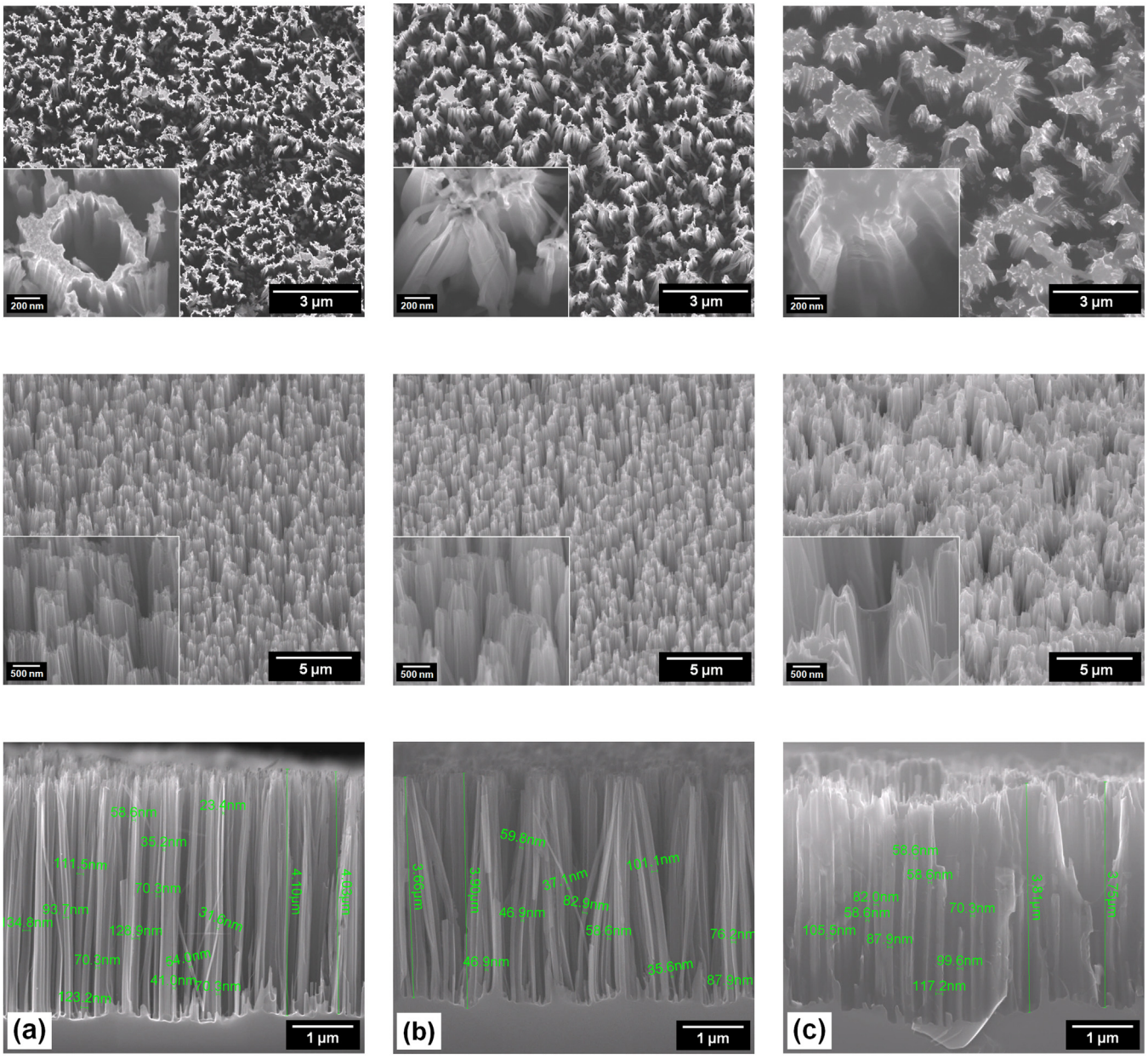

Fig. 2. Morphological examination of the (a) SiNWs; (b) SiNWs functionalized with APTES and GAD; (c) Si NWs covered with SU-8. The upper row depicts the in-plane view with high-resolution details, the middle row illustrates the 60° tilted images with representative micrographs, whereas the lower row shows the cross-section measurements of the configured Si substrate.

conditions compared with mismatches. A $*p < 0.05$ was deemed indicative of a statistically significant difference for these tests and is mentioned as $*p < 0.05$, $**p < 0.01$, and $***p < 0.001$ – significance levels for F statistics.

To further assess the quality of the developed microarray supports, we compared the signal-to-both-standard-deviations ratio (SSDR) using the calculation method reported [53]. The SSDRs of the ***GAD/SiNWs*** and ***SU-8/SiNWs*** were related to the ones obtained on aldehyde-modified commercial glass support (***REF***).

3. Results and discussion

3.1. Characterization of the 3D-modified microarray support

Extended surface and in-depth examination was conducted to assess the morphological changes exhibited by the SiNWs substrate after APTES-GAD and SU-8 functionalization. In Fig. 2, representative areas are illustrated along with high-resolution details intended for an accurate depiction of the 3D supports prepared for DNA probe immobilization. The in-plane view of the nanostructured support shows the natural bundling tendency of SiNWs, due to their high aspect ratio and surface tension generated by the evaporation of the liquid media involved in the fabrication procedure [54,55]. Adding the functional layers intensifies this process, as a result of the viscous material accumulation on the tips of the nanowires [56–58] and on the length of their exposed regions. The functionalization with APTES-GAD gathers the peaks of the nanowires and covers a significant portion of their length, as seen in the SEM micrograph. In addition, SU-8 not only encapsulates large nanowire groups into a polymeric mass, but, during the polymerisation process it forms bridges between adjacent blocks increasing the active surface, as indicated by the image acquired after tilting the sample. The cross-section investigation certifies the modification of the nanostructured Si substrate by functionalization and allows the measurement of nanowires (between 30 and 70 nm in diameter and ~ 4 μm

in length). Compared to the uncoated control sample, we observed a small reduction in thickness of the SiNWs layer after the functionalization step, explained by the clustering process mentioned above.

Complementary to the visual characterization, EDX analysis (Energy Dispersive X-ray spectroscopy) was performed for the accurate depiction of the specific elemental composition, revealing the presence of C, N and O related to APTES-GAD, and the C and O peaks associated with the SU-8 coating, respectively (Fig. S1, Supporting Information).

3.2. Immobilization mechanism

There are two factors that depend on the efficient recognition of the tethered probes by target DNA: the concentration of tethered probe has to be optimal to avoid crowding effect and steric hindrance, and the probes have to be oriented ideally in an upright position [59]. The use of a 3D configuration should eliminate the possibility of crowding effect and steric hindrance, and thus it increases the hybridization efficiency. The tendency of ssDNA and dsDNA molecules is to swing, bend or twist in the solvent towards the interface [60], but in the case where DNA probes have an NH_2 modification on 3′ or 5′ end, they provide covalent attachment with the surface-specific functional moieties, favouring the vertical orientation of DNA probes towards the surface and an efficient hybridization of ssDNA [61]. Our DNA probes had a 5′-NH_2-C6 linker which interacts with the aldehyde and epoxy-modified substrates, favouring the vertical orientation in relation to the surface, in accordance with Wong and Pettitt's [62] simulations on neutral epoxy-based monolayer indicating that the molecules tilt to 55° and back to the upright position, while the 5′-NH_2-C6 linker remains extended. Based on the SEM/EDX analyses, we expect in our cases to have slightly different orientation of the DNA probes. While in the case of APTES-GAD functionalization, the DNA molecules go deep into the 3D matrix and are immobilized quasi-vertical on the walls created by the grouping SiNWs, the SU-8 bridges restrict the in-depth DNA penetration and keep the molecules in vicinity of the surface, becoming more accessible for the hybridization process and favouring an increased sensitivity in detection. Fig. 3 illustrates the immobilization mechanisms on 3D Si based platforms modified with APTES-GAD (*GAD/SiNWs*) and with SU-8 (*SU-8/SiNWs*), respectively. In the first case, the Schiff base reaction between aldehyde and amine groups enables the covalent attachment of amine-modified DNA on 5′-end on SiNWs support, leading to a high binding strength and less random immobilization – Fig. 3(a). When SU-8 is coating the SiNWs, S_N2 type II nucleophilic substitution is promoted between the epoxy rings and the amine [63], ensuring superior binding strength and stability of the tethered probes [28] – Fig. 3(b).

3.3. Investigation of detection specificity over time

The probes' stability and specificity are essential properties for homemade microarrays targeting the commercial implementation. The few existing studies approached the short-term stability (up to 16 h) of unchanged and amine-modified probes printed on acid-washed or silanized surfaces [64], or up to 42 days evaluation of antibody arrays prior to data processing [65]. We periodically analysed the printed arrays on the 3D Si-based platforms (***GAD/SiNWs*** and ***SU-8/SiNWs***) by taking the commercial glass support as reference (***REF***) up to 21 days, probing the DNA attachment accuracy and the hybridization efficiency. Besides the scrutiny of fluorescent microarray images, the histograms and coefficients of variation were analysed to certify the stability over time. Furthermore, the graphical analyses were correlated with ANOVA statistics to demonstrate the detection specificity of highly stable oligonucleotides.

Resulting microarray optical images reveal significant differences between the spots obtained for each support type. Thus, the aldehyde-modified commercial glass substrate yields after 1 day of incubation good quality spots, with regular shapes and intensities, with diameters around 250 μm, larger than the pin tips (Fig. S3 **(a)**). After 21 days, a morphological alteration appears, caused by Marangoni and "coffee-ring" effects [66] (Fig. S3 **(b)**). The spot size is correlated with the wettability of the surface, the aldehyde-modified commercial support exhibiting hydrophilic characteristics with a mean contact angle of 74.3° (Fig. S2 **(a)**). The spot morphology and hybridization intensities on ***GAD/SiNWs*** platform are acceptable after 1 day, with an obvious decrease in signal intensity after 21 days of storage (Fig. S4). Higher diameters are obtained (~ 360 μm) due to the capillary diffusion of the immobilization solution containing single-stranded DNA probes and hybridization solution containing target oligonucleotides among the SiNWs [34], confirmed by the contact angle mean (76°), standard deviation (36°) and its reduction in time (Fig. S2 **(b)** and **(d)**). In contrast, the fluorescence images corresponding to ***SU-8/SiNWs*** after 1 and 21 days of storage disclosed uniform intensities and good spot morphologies besides smaller spot diameters (Fig. S5), principally due to the support's surface hydrophobicity, confirmed by the mean contact angle θ of 101° (Fig. S2 **(c)**). Their size is approximately 200 μm, close to the pin footprint, confirming the suitability of this type of surface functionalization in the development of experimental arrays close to the designed ones.

The signal-to-noise ratio (SNR) is widely used in microarray to measure the level of fluorescent signal related to hybridization, excluding the background noise [67,68]. The values of signal-to-both-standard-deviations ratio (SSDR) were calculated using Eq. 1 (Supplementary Information) and the results illustrated in Fig. 4 show on the one hand that the ***REF*** and ***SU-8/SiNWs*** microarray supports exhibit similar values, with improved stability over time for the latter, where the SSDR value decreases only by 10%. On the other hand, ***GAD/SiNWs*** presented the best SSDR values, 1.949 after 1 day and 1.803 after 21 days of storage, respectively, consistent with our previous results reported for fewer replicates [34], which are probably determined by the enlarged areas of microarray spots.

3.3.1. Analysis of PM probes stability over time

Following the blocking and washing steps, the stability of the PM probes was evaluated by hybridizing the slides after 1 day and 21 days of incubation at 4 °C. The graphical representation of normalized signal intensities was correlated with the average hybridization fluorescent intensities ($\bar{I}$), the standard deviations (σ) and coefficients of variation (CV), as presented in Fig. 5.

The histogram corresponding to ***REF*** support depicts the overlaid distributions of the signal intensities assessed after 1 and 21 days. For ***GAD/SiNWs***, the peaks of the distributions are off-centred with significant left skewing emerged after 21 days. Superior grouping tendency was observed for ***SU-8/SiNWs***, slightly left-shifted after 1 day of incubation, but greatly improved after 21 days. This fact has demanded a supplementary evaluation of middle intervals to confirm the long term stability, hence 4 days and 8 days were selected for investigations (Fig. S6, Supporting Information). The additional statistical analyses confirm this improving trend, showing two overlapped normal distributions (Fig. S7, Supporting Information).

The mean signal intensities ($\bar{I}$) were calculated using Eqs. (2) and (3) (Supporting information) for all the substrates and revealed that the highest hybridization signal intensities were obtained for ***REF*** with $\bar{I}_{1\,day} = 4.427$ and $\bar{I}_{21days} = 4.463$, followed by ***SU-8/SiNWs*** with $\bar{I}_{1\,day} = 4.409$ and $\bar{I}_{21days} = 4.140$, and by ***GAD/SiNWs*** with $\bar{I}_{1\,day} = 4.359$ and $\bar{I}_{21days} = 3.852$. The increase of average intensity calculated for the ***REF*** microarray is visually confirmed by simple comparison of the optical images (Fig. S3), where the saturation effect induced by the coffee-ring build-up was evident.

The standard deviations (σ) for 1 day and 21 days of storage were calculated according to Eqs. 4 and 5 (Supporting Information). The average quality of the spots in the case of commercial substrate is not substantially affected, the spreading of the results leading to values of $\sigma_{1\,day} = 0.081$ and $\sigma_{21days} = 0.099$ (Fig. 5**(a)**). Different results were obtained for the homemade supports: while the degree of preservation

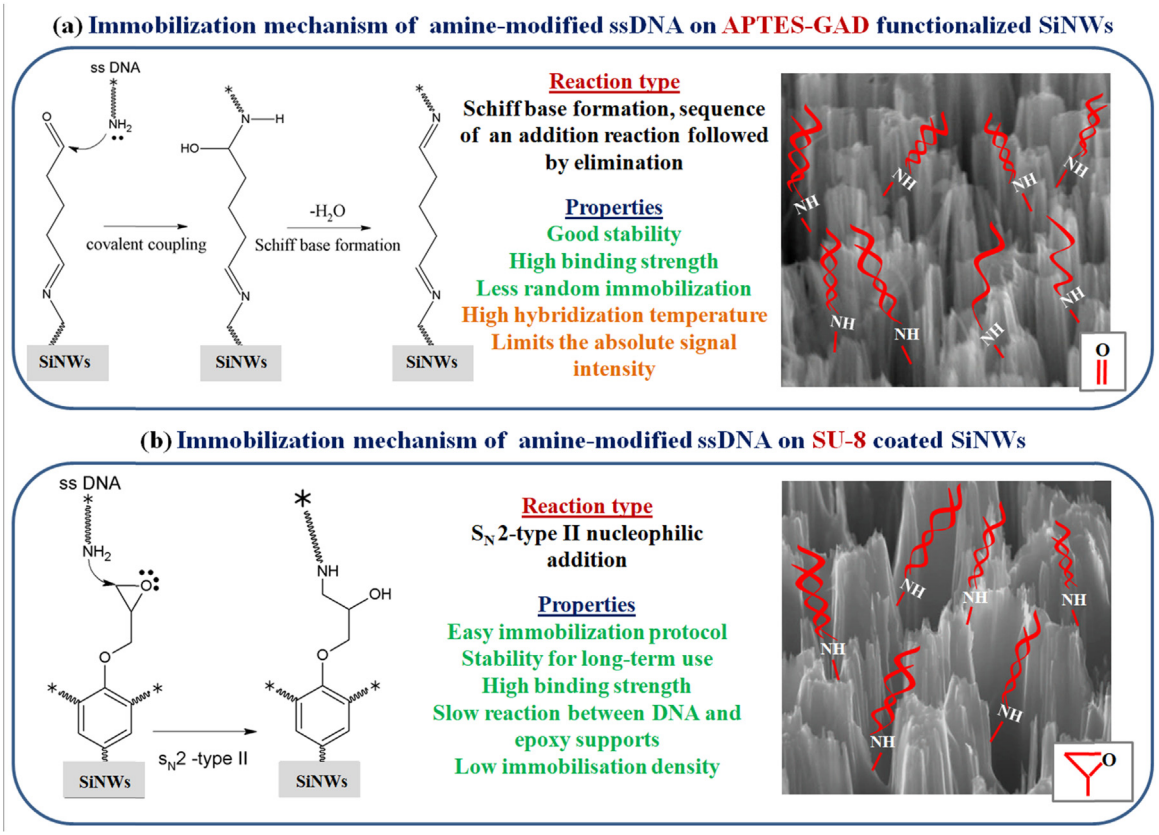

Fig. 3. Schematic illustration of the immobilization mechanisms of NH_2 – modified probe DNA on a) *GAD/SiNWs* and on b) *SU-8/SiNWs*.

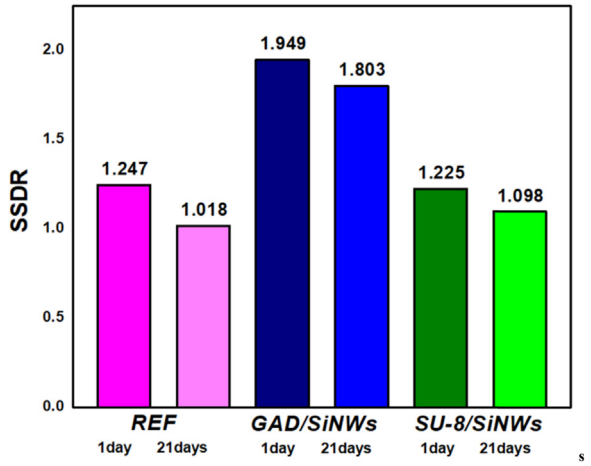

Fig. 4. Measurement of signal to both standard deviations ratio for the three types of biochips, after one day and twenty one days of printed slide incubation.

for ***GAD/SiNWs*** is initially $\sigma_{1\,day} = 0.153$ and suffers a decrease with time to $\sigma_{21days} = 0.256$ (Fig. 5**(b)**), the ***SU-8/SiNWs*** presents an opposing behaviour, where standard deviations improve from $\sigma_{1\,day} = 0.248$ to $\sigma_{21days} = 0.115$ (Fig. 5**(c)**).

The reproducibility of hybridized spots on the developed platforms is mainly given by the coefficient of variation (CV), calculated using Eq. 6 (Supporting Information). A value of CV smaller than 10% is in general acceptable, denoting better calculation accuracy when more technical replicates are involved [69–71]. All our analysed microarrays presented coefficients lower than 7%, reflecting the performance of the assay which guarantees the consistency of the manufacturing process. As expected, the highest stability over time was exhibited by ***REF*** with CV after 1 day ($CV_{1\,day}$) = 1.8% and CV after 21 days (CV_{21days}) = 2.2%. Inferior value of this coefficient was calculated for ***GAD/SiNWs*** after 1 day ($CV_{1\,day}$ = 3.5%) and it got even worse after 21 days, reaching CV_{21days} = 6.6%, anticipated by the skewed data distribution with disparate bimodal peaks. These findings can be associated with the removal of APTES/GAD/hybridized DNA layers caused by the hydrolytic instability of APTES after preserving the slides at 4 °C, in atmosphere with high humidity [72,73]. Analyzing the new ***SU-8/SiNWs*** configuration data, we obtained a coefficient that was, after 21 days, only slightly higher than the ones calculated for commercial slides, i.e. CV_{21days} = 2.8%.

3.3.2. Statistical investigation of the mismatch detection capabilities over time

A control experiment was performed by spotting all supports with negative controls, PM probe types, probes having C > A stable mismatch and with probe sequences containing two mismatches (CG > AA). The commercial glass support was taken as reference (***REF***) and single crystalline silicon surface modified with APTES-GAD and SU-8 (***GAD/Si*** and ***SU-8/Si***) was included for a comparative view with the 3D Si-based platforms (***GAD/SiNWs*** and ***SU-8/SiNWs***). One-way ANOVA test with Tukey's HSD post-hoc correction was performed on all substrates used for control experiments to assess the discrimination accuracy between the hybridized probes. The signal intensities normalized according to Eq. 2 (Supporting Information) were taken into consideration for PM probes in comparison with the MM probes (Fig. 6).

No fluorescent hybridized spots could be observed for negative controls which had been spotted and attached on all types of support. In Fig. S8 from Supporting Information, the pin features are clearly observed on the SiNWs, where the negative controls were tethered. The graphical analysis of ***REF*** shows statistical discrimination between PM, C > A and CG > AA mismatched probes (***p < 0.0001) (Fig. 6**(a)**). The statistical analysis of hybridization results on *GAD/Si* shows

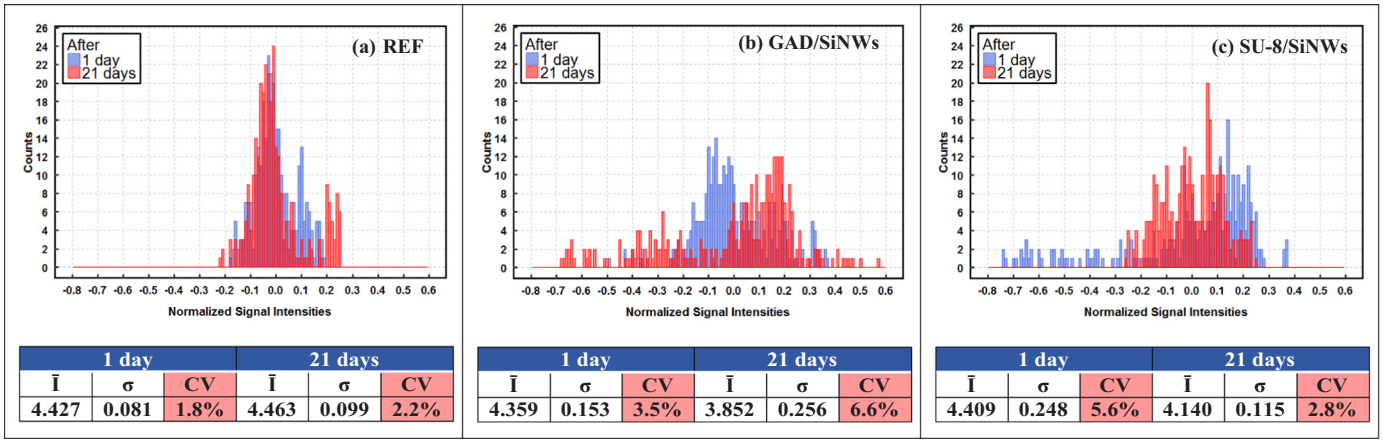

	1 day			21 days	
	Ī	σ	CV	Ī	σ	CV
(a) REF	4.427	0.081	1.8%	4.463	0.099	2.2%
(b) GAD/SiNWs	4.359	0.153	3.5%	3.852	0.256	6.6%
(c) SU-8/SiNWs	4.409	0.248	5.6%	4.140	0.115	2.8%

Fig. 5. Evaluation of the stability over time of surface-attached PM probes on: (a) commercial glass slide – *REF*; (b) glutaraldehyde-functionalized SiNWs – *GAD/SiNWs*; (c) SiNWs coated with SU-8 – *SU-8/SiNWs*, coupled with descriptive statistics for each type of substrate.

significant discrimination between PM and CG > AA probes (***p < 0.0001), whereas, the signal intensity higher for C > A (3.631) than PM (3.521) makes the ***GAD/Si*** an inaccurate detection platform (Fig. S9**(a)**, Supporting information). By analogy, the hybridization results on ***GAD/SiNWs*** revealed enhanced signal intensities (Fig. 6**(b)**), 4.198 instead of 3.521 on ***GAD/Si*** for PM, and statistical discrimination between all probe types (***p < 0.0001), although the average intensity of C > A (4.137) is slightly lower that PM.

On both ***SU-8/Si*** (Fig. S9 **(b)**, Supporting information) and ***SU-8/SiNWs*** (Fig. 6**(c)**), superior results were obtained in terms of detection specificity (***p < 0.0001), with a coefficient of variation equal to 2.16% of hybridized PM on ***SU-8/Si*** and 1.24% on ***SU-8/SiNWs***. The CG > AA probes have shown strong duplex destabilization when attached onto SU-8, as the fluorescent signal could not be clearly discerned from background and extracted for data analysis, whereas on the surfaces exposing aldehyde active moieties, the sequence with two mismatches could be detected, having the lowest hybridization signal intensity. Based on these findings, it was clear that not only the nanostructured surface, but also the functional groups play a major role in the accuracy of DNA detection, with a better hybridization specificity due to the higher reactivity of epoxy groups from SU-8 [74].

The ***REF***, ***GAD/SiNWs*** and ***SU-8/SiNWs*** slides spotted with PM, C > A and C > T mismatch types and hybridized have also been analysed after data extraction, normalization and outliers' removal by one-way ANOVA to assess the discrimination accuracy between the three types of hybridized probes. The normalized signal intensities were taken into consideration for PM probes in comparison to the MM probes (Fig. 7).

The graphical analysis of ***REF*** hybridization data after 1 day of incubation depicted in Fig. 7**(a1)** showed statistical discrimination between PM and C > T probes (***p < 0.0001), and also between C > A and C > T probes (***p < 0.0001). While the difference between PM and C > A is not statistically significant (ns 0.0675), the discrepancy was accentuated after 21 days, when although the difference PM vs. C > A could be considered significant, the higher hybridization signal of C > A probes made the analysis unreliable (red highlighted text in the table associated to Fig. 7**(a2)**. This behaviour might be determined by the predilection of C > A to generate stable A/G DNA duplexes after hybridization, having equal or higher signal intensity than C/G DNA duplex [75,76].

The same situation was found on ***GAD/SiNWs*** platform regarding the differences between the C > A and PM hybridized probes, both after 1 day and after 21 days of storage. If initially the coefficient value was reliable, its alteration was noticed also for C > T and PM after 21 days. Actually, it is notable that all the 'p' values become sub-standard after long-time storage.

Great specificity is achieved on ***SU-8/SiNWs*** biochip, revealing good distinction between the PM hybridized probes and C > A, C > T hybridized oligonucleotides (***p < 0.0001) after 1 day of incubation, with a slight difference (ns 0.9844) between the two mismatch types. An opposite behaviour in time could be observed for the last type of platform. Interestingly, the quality of mismatch detection on SU-8 coated substrate improved, showing good distinction between PM and MM probes, and also statistical differences between C > A and C > T

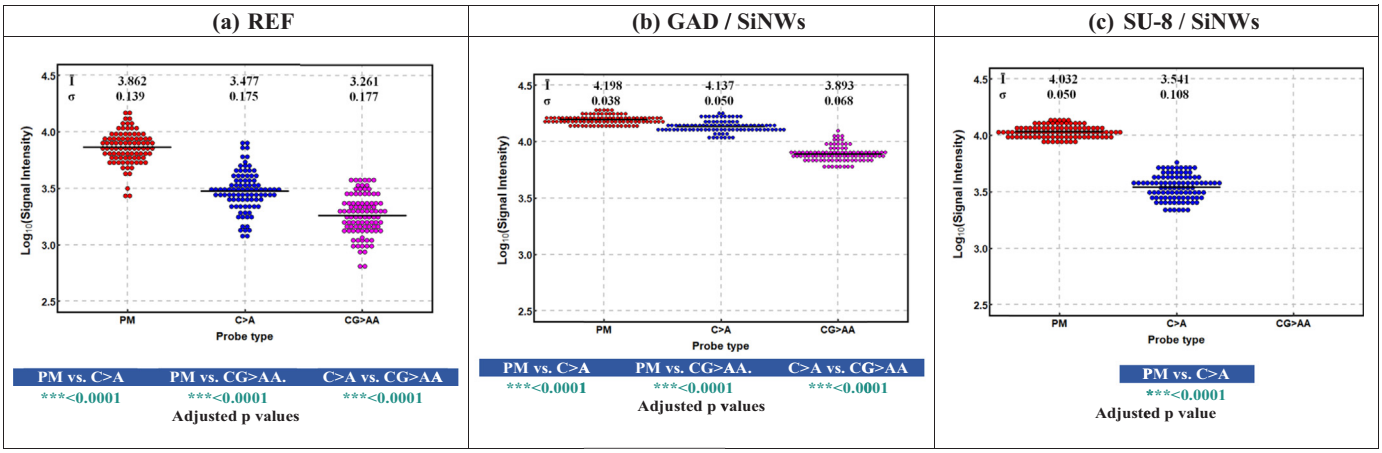

Fig. 6. Evaluation of the hybridization signal intensity differences between PM probes and the probes containing one (C > A) and two mismatches (CG > AA) on (a) commercial glass slide – *REF*; (b) glutaraldehyde-functionalized SiNWs – *GAD/SiNWs*; (c) SiNWs coated with SU-8 – *SU-8/SiNWs* correlated with statistical analysis.

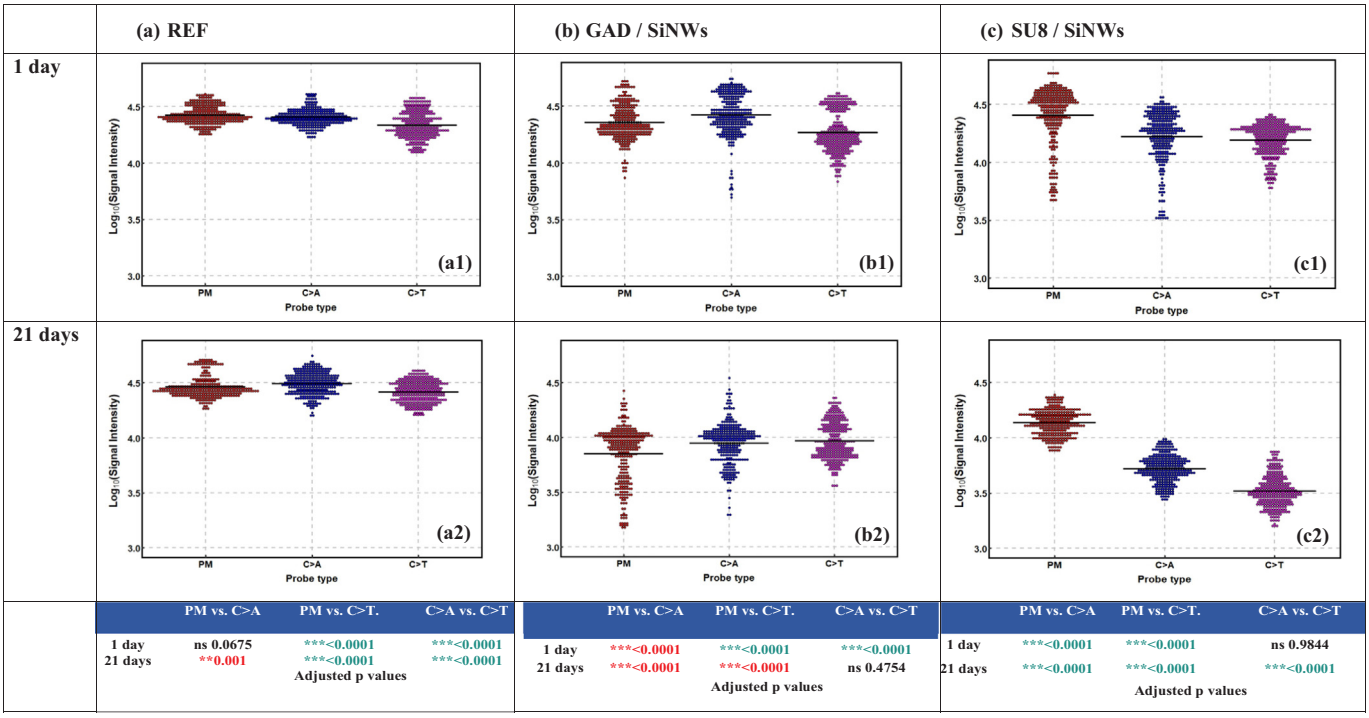

Fig. 7. Assessment of the signal intensity trends between the PM probe and the mismatches represented by C > A probe and C > T probe on (a) commercial glass slide – *REF*; (b) glutaraldehyde-functionalized SiNWs – *GAD/SiNWs*; (c) SiNWs coated with SU-8 – *SU-8/SiNWs* after 1 day and 21 days of incubation correlated with one way ANOVA analysis with Tukey's HSD post tests for 50 μM probe sequences diluted in Na_2HPO_4 hybridized with 10 μM target molecules.

fluorescent hybridization intensities (***$p < 0.0001$). Thus, although low immobilization density and slow reaction between DNA and epoxy supports were reported in the literature [28], our study emphasizes the tendency of the tethered probes to stabilize over time and to allow the discrimination between the most stable mismatches of *BRCA1*.

4. Conclusions

We presented the manufacturing of a stable SU-8 coated SiNWs biochip for enhanced mismatch detection, with hydrophobic properties leading to an average spot size very close to the imprint area of the pin tips. Consequently, the new platform allows the implementation of high density arrays addressed to end users engaged in detection of SNPs and various genotyping applications.

The uniform distribution of the probes increases the hybridization efficiency and consequently the detection specificity of single base mismatches. The statistical analyses conducted on 320 technical replicates/probe type indicate that the uniform SU-8 coverage of the SiNWs substrate in regard with both aldehyde-modified commercial slides and SiNWs-based homemade substrates with standard APTES-GAD functionalization improves the parameters which are related to the reproducibility of hybridization process. Uniquely, our comprehensive statistical approach highlighted the tendency of the tethered probes on ***SU-8/SiNWs*** platforms to stabilize over time, confirmed by the improvement of the calculated coefficient of variation up to 2.8% after 21 days. The capability of the new microarray support to allow detection of the highly stable mismatch types is remarkable, with significance levels between the different types of hybridized DNA probes of ***$p < 0.0001$, even after long storage period. Thus, we demonstrated that the use of a 3D architecture on Si and a simplified surface modification process with epoxy groups correspond to a reliable and inexpensive solution to achieve discrimination between the most stable mismatches of *BRCA1*. Real DNA samples will be involved in future experiments, as a final step in manufacturing an accurate diagnostics instrument.

Acknowledgements

This work was financed by the Romanian Ministry of Education and Research through the contract MiMoSa no. 36/2017.

Conflict of interest statement

The authors report no conflicts of interest. The authors alone are responsible for the content and writing of this articles.

Appendix A. Supporting information

Supplementary data associated with this article can be found in the online version at http://dx.doi.org/10.1016/j.talanta.2018.03.095.

References

[1] Y.H. Kim, J.R. Pollack, Microarray analysis of the physical Genome, Methods Mol. Biol. 556 (2009) 21–32.
[2] S.C. Sealfon, T.T. Chu, 2011. RNA and DNA microarrays in: Khademosseini, A., Suh, K.Y., Zourob, M. (Eds.) Biological Microarrays, Methods in molecular biology, Clifton, N.J, 671,pp. 1–32.
[3] T. LaFramboise, Single nucleotide polymorphism arrays: a decade of biological, computational and technological advances, Nucleic Acids Res. 37 (2009) 4181–4193.
[4] H.Y. Mun, A. Girigoswami, C. Jung, D.Y. Cho, H.G. Park, SNPs detection by a single-strand specific nuclease on a PNA zip-code microarray, Biosens. Bioelectron. 24 (2009) 1706–1711.
[5] A.C. Syvänen, Accessing genetic variation: genotyping single nucleotide polymorphisms, Nat. Rev. Genet. 2 (2001) 930–942.
[6] J. Chao, Z. Li, J. Li, H. Peng, S. Su, Q. Li, C. Zhu, X. Zuo, S. Song, L. Wang, L. Wang, Hybridization chain reaction amplification for highly sensitive fluorescence detection of DNA with dextran coated microarrays, Biosens. Bioelectron. 81 (2016) 92–96.
[7] R. Kargl, V. Vorraber, V. Ribitsch, S. Köstler, K. Stana-Kleinschek, T. Mohan, Selective immobilization and detection of DNA on biopolymer supports for the design of microarrays, Biosens. Bioelectron. 68 (2015) 437–441.
[8] H. Lahiri, S. Mishra, T. Mana, R. Mukhopadhyay, Discriminating unalike single nucleobase mismatches using a molecularly resolved, label-free, interfacial LNA-based assay, Analyst 141 (2016) 4035–4043.
[9] X. Piao, L. Sun, T. Zhang, Y. Gan, Y. Guan, Effects of mismatches and insertions on

discrimination accuracy of nucleic acid probes, Acta Biochim. Pol. 55 (2008) 713–720.
[10] A. Jayaraman, C.K. Hall, J. Genzer, Computer simulation study of probe-target hybridization in model DNA microarrays: Effect of probe surface density and target concentration, J. Chem. Phys. 127 (2007) (144912-1–144912-144914).
[11] R.M. Elder, A. Jayaraman, Simulation study of the effects of surface chemistry and temperature on the conformations of ssDNA oligomers near hydrophilic and hydrophobic surfaces, J. Chem. Phys. 140 (2014) (155103-1-155103-155116).
[12] K. Tsougeni, G. Koukouvinos, P.S. Petrou, A. Tserepi, S.E. Kakabakos, E. Gogolides, High-capacity and high-intensity DNA microarray spots using oxygen-plasma nanotextured polystyrene slides, Anal. Bioanal. Chem. 403 (2012) 2757–2764.
[13] B.R. Murthy, J.K.K. Ng, E.S. Selamat, N. Balasubramanian, W.T. Liu, Silicon nanopillar substrates for enhancing signal intensity in DNA microarrays, Biosens. Bioelectron. 24 (2008) 723–728.
[14] A. Kolchinsky, A. Mirzabekov, Analysis of SNPs and other genomic variations using gel-based chips, Hum. Mutat. 19 (2002) 343–360.
[15] R. Castagna, A. Bertucci, E.A. Prasetyanto, M. Monticelli, D.V. Conca, P.P. Sharma, F. Damin, M. Chiari, L. De Cola, R. Bertacco, Reactive microcontact printing of DNA probes on (DMA-NAS-MAP) co-polymer-coated substrates for efficient hybridization platforms, Langmuir 32 (2016) 3308–3313.
[16] A. Ressine, S. Ekström, G. Marko-Varga, T. Laurell, Macro-/nanoporous silicon as a support for high-performance protein microarrays, Anal. Chem. 75 (2003) 6968–6974.
[17] M. Simion, L. Ruta, C. Mihailescu, I. Kleps, A. Bragaru, M. Miu, T. Ignat, I. Baciu, Porous silicon used as support for protein microarray, Superlattices Microstruct. 46 (2009) 69–76.
[18] A. Yalçin, F. Damin, E. Özkumur, G. Di Carlo, B.B. Goldberg, M. Chiari, M.S. Unlü, Direct observation of conformation of a polymeric coating with implications in microarray applications, Anal. Chem. 81 (2009) 625–630.
[19] J.H. Lee, J.S. Kim, J.S. Park, W. Lee, K.E. Lee, S.S. Han, K.B. Lee, J. Lee, A three-dimensional and sensitive bioassay based on nanostructured quartz combined with viral nanoparticles, Adv. Funct. Mater. 20 (2010) 2004–2009.
[20] T. Bilgic, H.A. Klok, Surface-initiated controlled radical polymerization enhanced DNA biosensing, Eur. Polym. J. 62 (2015) 281–293.
[21] C. Oillic, P. Mur, E. Blanquet, G. Delapierre, F. Vinet, T. Billon, DNA microarrays on silicon nanostructures: optimization of the multilayer stack for fluorescence detection, Biosens. Bioelectron. 22 (2007) 2086–2092.
[22] S.G. Coombs, S. Khodjaniyazova, F.V. Bright, Exploiting the 3-Aminopropyltriethoxysilane (APTES) autocatalytic nature to create bioconjugated microarrays on hydrogen-passivated porous silicon, Talanta 177 (2018) 26–33.
[23] A.M. Gouda, N.K. Allam, M.A. Swillam, Efficient fabrication methodology of wide angle black silicon for energy harvesting applications, RSC Adv. 7 (2017) 26974–26982.
[24] S. Nichkalo, A. Druzhinin, A. Evtukh, O. Bratus, O. Steblova, Silicon nanostructures produced by modified MacEtch method for antireflective Si surface, Nanoscale Res. Lett. 12 (2017) 106.
[25] C. Zhang, S. Li, W. Ma, Z. Ding, X. Wan, J. Yang, Z. Chen, Y. Zou, J. Qiu, Fabrication of ultra-low antireflection SiNWs arrays from mc-Si using one step MACE, J. Mater. Sci. Mater. Electron. 28 (2017) 1–9.
[26] Z. Guo, J.-Y. Jung, K. Zhou, Y. Xiao, S. Jee, S. a. Moiz, J.-H. Lee, Optical properties of silicon nanowires array fabricated by metal-assisted electroless etching, New J. Phys. 7772 (2010) (77721C–77721C–7).
[27] M. Cretich, F. Damin, G. Pirri, M. Chiari, Protein and peptide arrays: recent trends and new directions, Biomol. Eng. 23 (2006) 77–88.
[28] S. Nimse, K. Song, M. Sonawane, D. Sayyed, T. Kim, Immobilization techniques for microarray: challenges and applications, Sensors 14 (2014) 22208–22229.
[29] M. Joshi, N. Kale, R. Lal, V.R. Rao, S. Mukherji, A novel dry method for surface modification of SU-8 for immobilization of biomolecules in Bio-MEMS, Biosens. Bioelectron. 22 (2007) 2429–2435.
[30] A. Deepu, V.V.R. Sai, S. Mukherji, Simple surface modification techniques for immobilization of biomolecules on SU-8, J. Mater. Sci.: Mater. Med. (2009) 25–28.
[31] D. Sethi, A. Kumar, R.P. Gandhi, P. Kumar, K.C. Gupta, New protocol for oligonucleotide microarray fabrication using SU-8-coated glass microslides, Bioconjugate Chem. 21 (2010) 1703–1708.
[32] R. Marie, S. Schmid, A. Johansson, L. Ejsing, M. Nordstr, H. Daniel, C. Bv, A. Boisen, M. Dufva, Immobilisation of DNA to polymerised SU-8 photoresist, Biosens. Bioelectron. 21 (2006) 1327–1332.
[33] R. Puchades, E. Peris, Photoattachment of thiolated DNA probes on SU-8 spin-coated Blu-ray disk surfaces for biosensing, J. Mater. Chem. B 1 (2013) 6245–6253.
[34] M. Banu, M. Simion, A.C. Ratiu, M. Popescu, C. Romanitan, M. Danila, A. Radoi, A.A. Ecovoiu, M. Kusko, Enhanced nucleotide mismatch detection based on a 3D silicon nanowire microarray, RSC Adv. 5 (2015) 74506–74514.
[35] M.C. Prosperi, S.L. Ingham, A. Howell, F. Lalloo, I.E. Buchan, D. Evans, Can multiple SNP testing in BRCA2 and BRCA1 female carriers be used to improve risk prediction models in conjunction with clinical assessment? BMC Med. Inform. Decis. Mak. 14 (2014) 1–11.
[36] A.C. Antoniou, J. Beesley, L. McGuffog, O.M. Sinilnikova, S. Healey, S.L. Neuhausen, Y.C. Ding, T.R. Rebbeck, J.N. Weitzel, H.T. Lynch, C. Isaacs, P.A. Ganz, G. Tomlinson, O.I. Olopade, F.J. Couch, X. Wang, N.M. Lindor, V.S. Pankratz, P. Radice, S. Manoukian, B. Peissel, D. Zaffaroni, M. Barile, A. Viel, A. Allavena, V. Dall'Olio, P. Peterlongo, C.I. Szabo, M. Zikan, K. Claes, Common breast cancer susceptibility alleles and the risk of breast cancer for BRCA1 and BRCA2 mutation carriers: implications for risk prediction, Cancer Res. 70 (2010) 9742–9754.
[37] D. Fanale, V. Amodeo, L.R. Corsini, S. Rizzo, V. Bazan, a. Russo, Breast cancer genome-wide association studies: there is strength in numbers, Oncogene 31 (2012) 2121–2128.
[38] R.L. Milne, A.C. Antoniou, Genetic modifiers of cancer risk for BRCA1 and BRCA2 mutation carriers, Ann. Oncol. 22 (2011) 11–17.
[39] C. Turnbull, S. Ahmed, J. Morrison, D. Pernet, A. Renwick, M. Maranian, S. Seal, M. Ghoussaini, S. Hines, C.S. Healey, D. Hughes, M. Warren-Perry, W. Tapper, D. Eccles, D.G. Evans, M. Hooning, M. Schutte, A. van den Ouweland, R. Houlston, G. Ross, C. Langford, P.D. Pharoah, M.R. Stratton, A.M. Dunning, N. Rahman, D.F. Easton, Genome-wide association study identifies five new breast cancer susceptibility loci, Nat. Genet. 42 (2010) 504–507.
[40] A. Granzhan, N. Kotera, M.-P. Teulade-Fichou, Finding needles in a basestack: recognition of mismatched base pairs in DNA by small molecules, Chem. Soc. Rev. 43 (2014) 3630–3665.
[41] Z. Huang, N. Geyer, P. Werner, J. de Boor, U. Gösele, Metal-assisted chemical etching of silicon: a review, Adv. Mater. 23 (2011) 285–308.
[42] M. Banu, A. Radoi, M. Simion, M. Kusko, Reproducible functionalization of silicon substrates intended for biomedical applications, in: Proceedings International Semicond. Conference CAS. 2016–Dec pp. 151–154, 2016.
[43] R. Martinez-Duarte, M. Madou, SU-8 Photolithography and Its Impact on Microfluidics, Microfluidics and Nanofluidics Handbook, (2011), pp. 231–268.
[44] ⟨http://www.ncbi.nlm.nih.gov/gene/672⟩.
[45] A. Kitts, S. Sherry, The Single Nucleotide Polymorphism Database (dbSNP) of Nucleotide Sequence Variation. ⟨http://www.ncbi.nlm.nih.gov/books/NBK21088/⟩.
[46] ⟨http://www.ncbi.nlm.nih.gov/snp?Db%BCs⟩, (Accessed January 2017).
[47] ⟨http://www.ncbi.nlm.nih.gov/projects/SNP/snp_ref.cgi?Rs=28897696⟩, (Accessed January 2017).
[48] M. Simion, L. Savu, A. Radoi, M. Miu, A. Bragaru, Detection of Human Papilloma viruses using nanostructurated silicon support in microarray technology, J. Nanosci. Nanotechnol. 11 (2011) 9102–9109.
[49] RStudio: Integrated development environment for R (Version 1. 0.136) [Computer software]. Boston, MA. Retrieved February 15 2017.
[50] R Core Team, R: a Language and Environment for Statistical Computing, R Foundation for Statistical Computing, Vienna, Austria, 2016 (URL), ⟨https://www.R-project.org/⟩.
[51] S. Draghici, Multiple Comparisons, in: Data Analysis Tools for DNA microarrays, Chapman and Hall/CRC Mathematical Biology and Medicine Series, Boca Raton, Florida, 2003.
[52] H. Wickham, ggplot2: Elegant Graphics for Data Analysis, Springer-Verlag, New York, 2009.
[53] Z. He, J. Zhou, Empirical evaluation of a new method for calculating signal-to-noise ratio for microarray data analysis, Appl. Environ. Microbiol. 74 (2008) 2957–2966.
[54] H. Han, J. Kim, H.S. Shin, J.Y. Song, W. Lee, Air-bridged ohmic contact on vertically aligned Si nanowire arrays: application to molecule sensors, Adv. Mater. 24 (2012) 2284–2288.
[55] M.K. Dawood, L. Zhou, H. Zheng, H. Cheng, G. Wan, R. Rajagopalan, H.P. Too, W.K. Choi, Nanostructured Si-nanowire microarrays for enhanced-performance bioanalytics, Lab Chip 12 (2012) 5016–5024.
[56] S.E. Saddow, Chapter 9: SiC Nanowire-Based Transistors for Electrical DNA Detection in Silicon Carbide Biotechnology: A Biocompatible Semiconductor for Advanced Biomedical Devices and Applications, Second ed., Elsevier, USA, 2016, pp. 261–306.
[57] M.L. Foglia, D.E. Camporotondi, G.S. Alvarez, S. Heinemann, T. Hanke, C.J. Perez, L.E. Diaz, M.F. Desimone, A new method for the preparation of biocompatible silica coated-collagen hydrogels, J. Mater. Chem. B. 1 (2013) 6283–6290.
[58] C.J. Robin, A. Vishnoi, K.N. Jonnalagadda, Mechanical behavior and anisotropy of spin-coated SU-8 thin films for MEMS, J. Micro. Syst. 23 (2014) 168–180.
[59] A.W. Peterson, L.K. Wolf, R.M. Georgiadis, Hybridization of mismatched or partially matched DNA at surfaces, J. Am. Chem. Soc. 124 (2002) 14601–14607.
[60] S. Monti, G. Prampolini, V. Barone, Interactions of nucleotide bases with decorated Si surfaces from molecular dynamics simulations, J. Phys. Chem. C 115 (2011) 9146–9156.
[61] J.I. Rashid, N.A. Yusof, The strategies of DNA immobilization and hybridization detection mechanism in the construction of electrochemical DNA sensor: a review, Sens Biosensing Res. 16 (2017) 19–31.
[62] K.Y. Wong, B.M. Pettitt, Orientation of DNA on a Surface from Simulation, Biopolymers 73 (2004) 570–578.
[63] G. Nikolic, S. Zlatkovic, M. Cakic, S. Cakic, C. Lacnjevac, Z. Rajic, Fast fourier transform IR characterization of epoxy GY systems crosslinked with aliphatic and cycloaliphatic EH polyamine adducts, Sensors 10 (2010) 684–696.
[64] D.R. Call, D.P. Chandler, F. Brockman, Fabrication of DNA microarrays using unmodified oligonucleotide probes, Biotechniques 30 (2001) 368–379.
[65] A. Gerdtsson, L. Dexlin-Mellby, P. Delfani, E. Berglund, C. Borrebaeck, C. Wingren, Evaluation of solid supports for slide- and well-based recombinant antibody microarrays, Microarrays 5 (2016) 1–17.
[66] A.N. Rao, D.W. Grainger, Biophysical properties of nucleic acids at surfaces relevant to microarray performance, Biomater. Sci. 2 (2014) 436–471.
[67] H. Hong, Q. Hong, J. Liu, W. Tong, L. Shi, Estimating relative noise to signal in DNA microarray data. International journal of bioinformatics research and applications, Int. J. Bioinform. Res. Appl. 9 (2013) 433–448.
[68] D. Venet, V. Detours, H. Bersini, A measure of the signal-to-noise ratio of microarray samples and studies using gene correlations, PLoS One 7 (2012) 1–9.
[69] J.L. Calvi, F.R. Chen, V.B. Benson, E. Brindle, M. Bristow, A. De, S. Entringer, H. Findlay, C. Heim, E.A. Hodges, H. Klawitter, S. Lupien, H.M. Rus, J. Tiemensma, S. Verlezza, C.-D. Walker, D.A. Granger, Measurement of cortisol in saliva: a comparison of measurement error within and between international academic-research laboratories, BMC Res. Notes 10 (2017) 479.

[70] A.S. Glotov, E.S. Sinitsyna, M.M. Danilova, E.S. Vashukova, J.G. Walter, F. Stahl, V.S. Baranov, E.G. Vlakh, T.B. Tennikova, Detection of human genome mutations associated with pregnancy complications using 3-D microarray based on macroporous polymer monoliths, Talanta 147 (2016) 537–546.
[71] L.M. Strambini, A. Longo, S. Scarano, T. Prescimone, I. Palchetti, M. Minunni, D. Giannessi, G. Barillaro, Self-powered microneedle-based biosensors for pain-free high-accuracy measurement of glycaemia in interstitial fluid, Biosens. Bioelectron. 66 (2015) 162–168.
[72] M. Zhu, M.Z. Lerum, W. Chen, How to prepare reproducible, homogeneous, and hydrolytically stable aminosilane-derived layers on silica, Langmuir (2012) 416–423.
[73] N. Aissaoui, L. Bergaoui, J. Landoulsi, J.F. Lambert, S. Boujday, Silane layers on silicon surfaces: mechanism of interaction, stability, and influence on protein adsorption, Langmuir 28 (2012) 656–665.
[74] M.D. Sonawane, S.B. Nimse, Surface modification chemistries of materials used in diagnostic platforms with biomolecules, J. Chem. 2016 (2016) 1–19.
[75] Y. Li, G. Zon, W.D. Wilson, NMR and molecular modeling evidence for a G.A mismatch base pair in a purine-rich DNA duplex, Proc. Natl. Acad. Sci. USA 88 (1991) 26–30.
[76] H.T. Allawi, J. SantaLucia, Nearest neighbour thermodynamic parameters for internal G·A mismatches in DNA, Biochemistry 37 (1998) 2170–2179.